PHYSICAL REVIEW C, VOLUME 65, 031901(R)

Centrality dependence of charged particle multiplicity at midrapidity in Au+Au collisions at $\sqrt{s_{NN}}=130$ GeV

B. B. Back,[1] M. D. Baker,[2] D. S. Barton,[2] R. R. Betts,[6] R. Bindel,[7] A. Budzanowski,[3] W. Busza,[4] A. Carroll,[2] M. P. Decowski,[4] E. Garcia,[7] N. George,[1] K. Gulbrandsen,[4] S. Gushue,[2] C. Halliwell,[6] G. A. Heintzelman,[2] C. Henderson,[4] R. Hołyński,[3] D. J. Hofman,[6] B. Holzman,[6] E. Johnson,[8] J. L. Kane,[4] J. Katzy,[4] N. Khan,[8] W. Kucewicz,[6] P. Kulinich,[4] W. T. Lin,[5] S. Manly,[8] D. McLeod,[6] J. Michałowski,[3] A. C. Mignerey,[7] J. Mülmenstädt,[4] R. Nouicer,[6] A. Olszewski,[2,3] R. Pak,[2] I. C. Park,[8] H. Pernegger,[4] C. Reed,[4] L. P. Remsberg,[2] M. Reuter,[6] C. Roland,[4] G. Roland,[4] L. Rosenberg,[4] P. Sarin,[4] P. Sawicki,[3] W. Skulski,[8] S. G. Steadman,[4] G. S. F. Stephans,[4] P. Steinberg,[2] M. Stodulski,[3] A. Sukhanov,[2] J. -L. Tang,[5] R. Teng,[8] A. Trzupek,[3] C. Vale,[4] G. J. van Nieuwenhuizen,[4] R. Verdier,[4] B. Wadsworth,[4] F. L. H. Wolfs,[8] B. Wosiek,[3] K. Woźniak,[3] A. H. Wuosmaa,[1] and B. Wysłouch[4]

(PHOBOS Collaboration)

[1]*Physics Division, Argonne National Laboratory, Argonne, Illinois 60439-4843*

[2]*Chemistry and Collider-Accelerator Departments, Brookhaven National Laboratory, Upton, New York 11973-5000*

[3]*Institute of Nuclear Physics, Kraków, Poland*

[4]*Laboratory for Nuclear Science, Massachusetts Institute of Technology, Cambridge, Massachusetts 02139-4307*

[5]*Department of Physics, National Central University, Chung-Li, Taiwan*

[6]*Department of Physics, University of Illinois at Chicago, Chicago, Illinois 60607-7059*

[7]*Department of Chemistry and Biochemistry, University of Maryland, College Park, Maryland 20742*

[8]*Department of Physics and Astronomy, University of Rochester, Rochester, New York 14627*

(Received 18 May 2001; published 5 February 2002)

We present a measurement of the pseudorapidity density of primary charged particles near midrapidity in Au+Au collisions at $\sqrt{s_{NN}}=130$ GeV as a function of the number of participating nucleons. The pseudorapidity density, $dN_{ch}/d\eta|_{|\eta|<1}/(\frac{1}{2}\langle N_{part}\rangle)$, rises from 2.87 ± 0.21 in peripheral events ($\langle N_{part}\rangle\sim83$) to 3.45 ±0.18 in central events ($\langle N_{part}\rangle\sim353$), which is $53\pm8\%$ higher than $p\bar{p}$ collisions at a similar center-of-mass energy. This is consistent with an additional contribution to charged particle production that scales with the number of binary nucleon-nucleon collisions (N_{coll}).

DOI: 10.1103/PhysRevC.65.031901 PACS number(s): 25.75.Dw

Collisions of gold nuclei at the Relativistic Heavy Ion Collider (RHIC) provide a unique opportunity to study particle production in nuclear collisions at the highest available energies. In a previous publication [1], the PHOBOS Collaboration presented results on the energy dependence of the pseudorapidity density of charged particles, $dN_{ch}/d\eta$, produced near midrapidity for central Au+Au collisions. It showed that this rises much faster with energy than in $p\bar{p}$ collisions at similar energies [2]. This has been explained by the increasing role of hard and semihard processes, which are described using perturbative QCD.

One way to control the ratio of hard to soft production at a fixed beam energy is to vary the impact parameter, or centrality, of the nuclear collisions. Soft processes, which produce the bulk of charged particles in pp and pA collisions, scale with the number of participating nucleons (N_{part}) in the collision [3,4]. Hard processes occur in the interactions between individual partons in the colliding nucleons and are expected to scale with the number of nucleon-nucleon collisions, N_{coll}. The contribution of both hard and soft processes to particle production leads to an expected scaling of $dN_{ch}/d\eta|_{\eta=0}$ as $A\times N_{part}+B\times N_{coll}$.

Data from the WA98 experiment at CERN [5] already indicate possible deviations from simple N_{part} scaling even at SPS energies ($\sqrt{s_{NN}}=17.2$ GeV). A stronger-than-linear dependence on N_{part} is observed, well described by a power-law, $dN_{ch}/d\eta|_{\eta=0}\propto N_{part}^{\alpha}$, with $\alpha=1.07\pm0.04$.

Theoretical models of particle production in RHIC collisions generally fall into two classes. The first incorporates the expected scaling mentioned above, using a Glauber model calculation [6] to determine the relationship between N_{part} and N_{coll} as a function of impact parameter. The HIJING model [7] as well as calculations by Kharzeev and Nardi (KN) [8] follow this ''two component'' approach. HIJING also incorporates jet quenching and nuclear shadowing which modifies the scaling, leading to a linear rise of the normalized multiplicity $dN_{ch}/d\eta/N_{part}$ versus N_{part}. KN do not include these additional effects, the only input parameters being the fraction of particle production from hard processes and the earlier PHOBOS result. This leads to a dependence of $dN_{ch}/d\eta$ on N_{part} similar to that measured by WA98.

The second class of calculations, based on parton saturation, predict a different dependence on the nuclear geometry. For example, the EKRT model [9], which incorporates a geometry-dependent saturation scale, predicts a near-constant dependence of $dN_{ch}/d\eta/N_{part}$ as a function of N_{part}. In Ref. [8], KN also perform a calculation based on parton saturation, including the evolution of the gluon structure function. They find that $dN_{ch}/d\eta/N_{part}$ scales as $\ln(Q_s^2/\Lambda^2)$, where Q_s^2 is the saturation momentum scale which depends on the impact parameter. Perhaps fortuitously, this latter calculation is in near-perfect agreement with the other KN result at $\sqrt{s_{NN}}=130$ GeV above $N_{part}\sim70$. This suggests that it may be difficult to distinguish the two-component and saturation scenarios except in the most peripheral events.

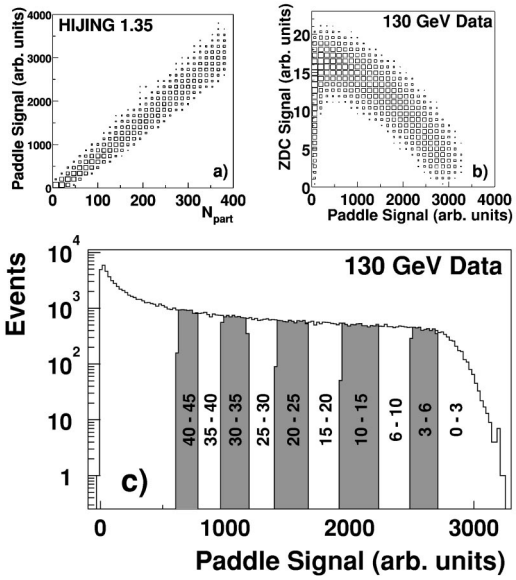

FIG. 1. (a) Simulated paddle signal as a function of the number of participants. (b) ZDC signal vs paddle signal for PHOBOS data at $\sqrt{s_{NN}}=130$ GeV. (c) Paddle signal with cuts selecting fractions of the estimated total inelastic cross section.

We present the results of a measurement of the charged particle multiplicity per participating nucleon pair near midrapidity, $dN_{ch}/d\eta|_{|\eta|<1}/(\frac{1}{2}\langle N_{part}\rangle)$, as a function of N_{part}. For this measurement, we used a subset of the full PHOBOS detector, which was partially described in Ref. [1].

To measure the charged particle multiplicity, we used two of the three silicon detector systems implemented in PHOBOS [10], each of which has different properties and thus different systematic effects on the data. The PHOBOS spectrometer ($SPEC$) used for the 2000 data consists of two arms, one with 16 ($SPECN$) and another with six layers ($SPECP$). The first six layers of each subdetector subtend $-1<\eta<2$ and $\Delta\phi<7°$ around $\phi=0$ ($SPECP$) and $\phi=180°$ ($SPECN$). The innermost of these layers has 1×1 mm^2 pads while the pads get narrower and taller as the distance from the event vertex increases. The PHOBOS vertex detector (VTX) consists of two sets ($VTXT/VTXB$) of two layers which are located above and below the beam (z) axis. Primarily designed to measure the vertex z position (z_{vtx}), the pads have very fine segmentation along z, but are larger in the x (horizontal) direction. For events with $z_{vtx}=0$, the detector covers $\Delta\phi\approx\pm22°$ around $\phi=90°$ and 270° and $\Delta\eta=\pm0.97$ around $\eta=0$.

The centrality of the collisions, from which we derive N_{part}, is primarily determined using the energy deposited by charged particles in two sets of paddle counters located at ±3.21 meters from the nominal interaction point along the beam axis, which subtend $3<|\eta|<4.5$. HIJING simulations [11] suggest that, on average, the paddle signal is monotonically related to the number of participants, as shown in Fig. 1(a). This has been verified by the PHOBOS data shown in Fig. 1(b), which shows an anticorrelation between the paddle signal and the signal from the zero-degree calorimeters (ZDCs) [12] which are located at ±18 m and measure the forward-going neutral spectator matter. Except for the most peripheral events, where fragment formation reduces the amount of forward-going neutral energy, this behavior is expected if the ZDC signal scales monotonically with $2A-N_{part}$.

TABLE I. For each centrality bin, based on percentile of the total cross section, we show the number of participants, the error-weighted average of the two measurements of $dN_{ch}/d\eta$, and the final result for $dN_{ch}/d\eta/(\frac{1}{2}\langle N_{part}\rangle)$, including the full error estimation.

	Measured		Derived
Bin(%)	$\langle dN_{ch}/d\eta\rangle$	$\langle N_{part}\rangle$	$dN_{ch}/d\eta/(\frac{1}{2}\langle N_{part}\rangle)$
0–3	610±24	353±11	3.45±0.18
3–6	550±22	329±9	3.34±0.16
6–10	474±18	291±8	3.25±0.16
10–15	399±16	252±8	3.16±0.16
15–20	336±13	215±7	3.12±0.16
20–25	277±11	180±6	3.08±0.17
25–30	227±9	149±6	3.03±0.18
30–35	185±7	122±5	3.00±0.18
35–40	149±6	102±5	2.91±0.20
40–45	120±5	83±4	2.87±0.21

As a consequence of the monotonic relationship between the paddle signal and N_{part}, fractions of the cross section as selected by the paddle signal [shown in Fig. 1(c)] correspond on average to the same fractions of the cross section selected by N_{part}. To account for the fluctuations of secondaries produced in the apparatus as well as of N_{part} itself, we actually calculate $\langle N_{part}\rangle$ for fractions of the cross section selected using a full simulation of the paddle response based on HIJING and GEANT. This has been done for each of ten bins in the most central 45% of the total cross section (shown in Table I). We find that for the PHOBOS setup, ignoring all sources of fluctuations leads to shifts in $\langle N_{part}\rangle$ of less than 2%.

A major source of experimental systematic error in the determination of $\langle N_{part}\rangle$ arises from uncertainty in the efficiency of our event selection procedure (described in Ref. [1]) for low-multiplicity events. We have estimated this by studying the frequency distribution of the number of hit paddle counters, which is sensitive to the most peripheral events, and comparing the results to Monte Carlo simulations. By performing the procedure with two different models (HIJING, RQMD [13]) we estimate a systematic error of 3% and an efficiency of 97%. Unfortunately, an error of as little as 3% leads to errors on $\langle N_{part}\rangle$ on the order of 5% for $N_{part}<100$. This uncertainty accounts for about half of the total systematic error on the final result described below.

It should be noted that the Glauber model calculation implemented in HIJING 1.35 uses a Monte Carlo approach. In this, nucleons are randomly distributed according to a Woods-Saxon distribution, and interactions occur with a probability proportional to the overlap of the Gaussian nucleon density profiles. This is very similar to the procedure used by the PHENIX Collaboration in a recent publication

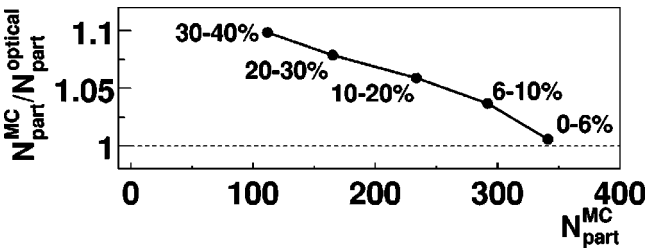

FIG. 2. Ratio of N_{part} calculated by HIJING (MC-based estimate of the full Glauber calculation) over N_{part} calculated by KN (optical approximation) vs HIJING. Each comparison is done for the same fraction of total cross section, as indicated next to the points.

[14]. A different approach is taken by KN [8,15], who use a numerical integration of the nuclear overlap function that should in principle give identical results as the Monte Carlo approach. However, it is well known that these calculations are done in the optical limit to make the integrals tractable. While this approximation is reasonable for expressing N_{ch} as a function of N_{part} or impact parameter, as is done in the KN calculations, it is known to be inaccurate for estimating the total inelastic cross section [16]. Thus, for the same fraction of cross section, it can be *expected* to give different results for $\langle N_{part} \rangle$ relative to a Monte Carlo approach. In fact, we have found that the two approaches do disagree, and moreover, cannot be brought into agreement by reasonable variation of the input parameters (e.g., radius and σ_{NN}). The ratio of N_{part} from HIJING (''MC'') over KN (''optical'') is shown in Fig. 2 as a function of N_{part} from HIJING.

Following the procedure described in [1], we have determined the charged particle multiplicity, $dN_{ch}/d\eta$, at midrapidity averaged over $|\eta|<1$. The technique is based on counting ''tracklets,'' which are three-point tracks consisting of two points and the measured event vertex. In this analysis, we have used combinations of five effective ''subdetectors'': layers 1 and 2 of *SPECP* and *SPECN*, layers 5 and 6 of *SPECP* and *SPECN*, and the full vertex detector. The large number of differently positioned detectors allowed us to control the effects of backgrounds and was used to check the consistency of our analysis technique.

For the spectrometer, the pseudorapidity η and azimuthal angle ϕ of all hits in two consecutive spectrometer layers were calculated relative to the primary event vertex. Tracklets were then constructed by combining pairs of hits in both layers for which the total angular distance $D=\sqrt{\delta\eta^2+\delta\phi^2}$ satisfies the condition $D<0.015$, where $\delta\eta$ and $\delta\phi$ are the deviations in pseudorapidity and azimuthal angle (in radians) of the two hits, respectively. If two tracklets share a hit, the one with the larger value of D is discarded. A similar tracklet finding algorithm was used for the vertex detector. Tracklets were chosen in the vertex detector as combinations of hits in the two detector layers with $|\delta\phi|<0.3$ and $|\delta\eta|<0.04$. We did not use the same measure D as for the spectrometer since the granularity in the vertex detector is substantially coarser in the ϕ direction.

To study the effect of combinatorial backgrounds, we analyzed the full data sample with the inner layers of each set of detectors rotated about the beam axis by 180°. While preserving the gross features of the events (e.g., flow), the tracklets extracted from this data set arise exclusively from random coincidences of two hits that satisfy our quality cuts. Outside of the cut region, we find that the distribution of track residuals (D for the spectrometer, $\delta\eta$ for the vertex) for the mixed-hit tracklets closely matches those obtained with the true detector geometry. By normalizing the two distributions outside the cuts, we thus obtain an estimate of the combinatorial background in the region of accepted tracklets.

The high segmentation of the spectrometer in both pseudorapidity and azimuthal angle leads to a small number of background tracklets, which is substantially larger for the vertex detector because of its larger pads. In both cases, the background level was found to scale with the number of occupied pads. In the spectrometer, the background varied from 1% to 15%, depending on occupancy. The final number of tracklets is corrected for this combinatorial background with the measured distribution, smoothed using a second-order polynomial. The coarser segmentation of the vertex detector leads to a larger contribution from combinatorial tracklets. However, since the scaling of the background with the number of occupied pads is similar in data and simulation, we use a global correction factor to take this into account. Making an explicit correction similar to the spectrometer has a negligible effect (less than 1%) on the final answer.

The proportionality factor α between the number of tracklets and the multiplicity of primary charged particles for $|\eta|<1$ was calculated using the results of simulations. Particles generated by HIJING were propagated through GEANT 3.21. The resulting simulated signals were smeared to account for detector resolution, and subjected to the same analysis chain as the real data.

The precise manner in which these proportionality factors were calculated and used is somewhat different in the spectrometer and vertex detectors. In the spectrometer, α was computed as a function of z_{vtx} and centrality. Since the spectrometer acceptance is forward of midrapidity, we only include tracklets within a fiducial cut of $0<\eta<1$. Using these proportionality factors, the raw number of tracklets was calculated using events in $-4<z_{vtx}<12$ cm. For each centrality and vertex bin, the background fraction, which depends on the number of occupied pads, was also averaged over the selected events and then subtracted from the average number of tracklets to obtain the final multiplicity. In the vertex detector, α was computed for tracklets in $|\eta|<1$ as a function of z_{vtx} (for $|z_{vtx}|<12$ cm) and N_{outer}, where N_{outer} is the number of hits in the outer vertex layer. This corrects for both the reconstruction efficiency and the combinatorial background. It is more difficult to distinguish these two effects in the vertex detector, which lacks the pointing accuracy of the spectrometer. The final estimate of $dN_{ch}/d\eta|_{|\eta|<1}$ was then determined in both cases by averaging over z_{vtx} in each centrality bin.

The systematic error for the spectrometer is dominated by the accuracy of the vertex determination and the efficiency of the tracklet reconstruction procedure and is estimated to be 3%. The uncertainty on the combinatorial background subtraction has been estimated to be 1%. Finally, the uncertainty in the effect of nonvertex backgrounds (which includes weak

decays) has been estimated to be less than 1%. Thus, we estimate an error of 4.5%, independent of centrality.

The vertex detector has larger systematic errors, due to its coarser segmentation in the x direction, which makes it less robust against contamination from nonvertex backgrounds, such as delta electrons and weak decays. By considering how the final result varies with changes in the quality cuts and event generator used, we estimate a final systematic error of 7.5%.

The final value of $dN_{ch}/d\eta|_{|\eta|<1}$ is based on an average of two separate measurements, one combining the four spectrometer measurements and one with the full vertex detector. Since the systematics are very different for the two different analysis techniques, we combine the two results weighted by the inverse of their total systematic error squared to obtain the final results, which are shown in Table I.

The scaled pseudorapidity density $dN_{ch}/d\eta|_{|\eta|<1}/(\frac{1}{2}\langle N_{part}\rangle)$ as a function of N_{part} is shown in Fig. 3, with $\langle N_{part}\rangle$ derived using HIJING. The two different sources of systematic error, one from the tracklet measurement and the other from the estimation of N_{part}, are combined in quadrature and shown as a band around the data points. The error on the participant estimation is based on the assumption that we may have misestimated the total cross section by 3%, our systematic error on this quantity. For comparison, we show an extrapolation of $\bar{p}p$ measurements to $\sqrt{s_{NN}}=130$ GeV using a procedure described in [2] (solid circle), as well as the PHOBOS measurement of the pseudorapidity density at midrapidity [1] (solid square). For the most central events, the multiplicity is $53\pm 8\%$ higher than the $\bar{p}p$ values. Our results are in good agreement with a recent PHENIX publication [14].

Three model comparisons are also shown. The HIJING model (solid curve) interpolates almost linearly between the $\bar{p}p$ point and the previous PHOBOS point [1]. Above this, we show the KN two-component calculation as a single dotted curve. Note that the absolute scale in this model was normalized to the PHOBOS value for the 6% most central events [8]. Finally, the saturation results of EKRT (dashed curve) are nearly constant as a function of N_{part}. The data

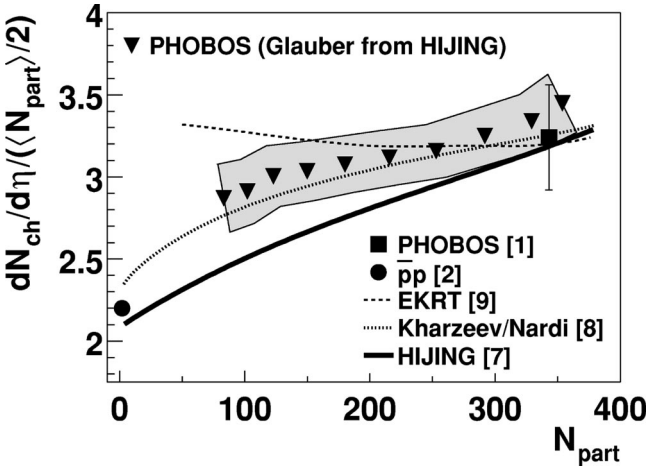

FIG. 3. The measured scaled pseudorapidity density $dN_{ch}/d\eta|_{|\eta|<1}/(\frac{1}{2}\langle N_{part}\rangle)$ is shown as a function of N_{part} (solid triangles), with N_{part} extracted using HIJING. The error band combines the error on $dN_{ch}/d\eta|_{|\eta|<1}$ and N_{part}. The solid circle is $\bar{p}p$ data from Ref. [2]. The solid square is from Ref. [1]. Theoretical calculations are shown from HIJING [7] (solid line), KN [8] (dotted curve) and EKRT [9] (dashed curve).

appear to disfavor the HIJING and EKRT results. However, they are consistent with the KN result which has the simple scaling expected by a Glauber model including contributions to charged particle production proportional to N_{part} and N_{coll}.

This work was partially supported by U.S. DOE Grant Nos. DE-AC02-98CH10886, DE-FG02-93ER40802, DE-FC02-94ER40818, DE-FG02-94ER40865, DE-FG02-99ER41099, W-31-109-ENG-38 and NSF Grant Nos. 9603486, 9722606, and 0072204. The Polish groups were partially supported by KBN Grant No. 2 P03B 04916. The NCU group was partially supported by NSC of Taiwan under Contract No. NSC 89-2112-M-008-024. We would like to thank A. Białas, W. Czyż, D. Kharzeev, K. Reygers, and K. Zalewski for helpful discussions.

[1] PHOBOS Collaboration, B.B. Back *et al.*, Phys. Rev. Lett. **85**, 3100 (2000).
[2] F. Abe *et al.*, Phys. Rev. D **41**, 2330 (1990).
[3] J.E. Elias *et al.*, Phys. Rev. D **22**, 13 (1980).
[4] A. Białas, B. Bleszyński, and W. Czyż, Nucl. Phys. **B111**, 461 (1976).
[5] WA98 Collaboration, M.M. Aggarwal *et al.*, Eur. Phys. J. C **18**, 651 (2001).
[6] R. J. Glauber, in *Lectures in Theoretical Physics*, edited by W. E. Brittin and L. G. Dunham (Interscience, New York, 1959), Vol. 1, 315, 1959.
[7] X.N. Wang and M. Gyulassy, Phys. Rev. Lett. **86**, 3496 (2001).
[8] D. Kharzeev and M. Nardi, Phys. Lett. B **507**, 121 (2001).
[9] K.J. Eskola, K. Kajantie, and K. Tuominen, Phys. Lett. B **497**, 39 (2001); K.J. Eskola, K. Kajantie, P. V. Ruuskanen, and K. Tuominen, Nucl. Phys. **B570**, 379 (2000).
[10] H. Pernegger *et al.*, Nucl. Instrum. Methods Phys. Res. A **419**, 549 (1998).
[11] X.N. Wang and M. Gyulassy, Phys. Rev. D **44**, 3501 (1991). We used HIJING V1.35 (April 1998) with standard parameter settings.
[12] C. Adler, A. Denisov, E. Garcia, M. Murray, H. Strobele and S. White, Nucl. Instrum. Methods Phys. Res. A **461**, 337 (2001).
[13] H. Sorge, Phys. Rev. C **52**, 3291 (1995).
[14] PHENIX Collaboration, K. Adcox *et al.*, Phys. Rev. Lett. **86**, 3500 (2001).
[15] D. Kharzeev, C. Lourenco, M. Nardi and H. Satz, Z. Phys. C **74**, 307 (1997).
[16] A. Białas (private communication); V. Franco and G.K. Varma, Phys. Rev. C **18**, 349 (1978).